Fine-structure-resolved electron collisions from chlorine atoms in the $(3p^{5})^{2}P_{3/2}^{o}$ and $(3p^{5})^{2}P_{1/2}^{o}$ states

Yang Wang, Oleg Zatsarinny, Klaus Bartschat, and Jean-Paul Booth

Finestructure-resolved electron collisions from chlorine atoms in the $(3p^5)^2P^o_{3/2,1/2}$ states

Yang Wang,[1, 2, *] Oleg Zatsarinny,[2, †] Klaus Bartschat,[2, ‡] and Jean-Paul Booth[3, §]

[1]*Center for Theoretical Atomic and Molecular Physics,*
Academy of Fundamental and Interdisciplinary Sciences,
Harbin Institute of Technology, Harbin, 150080, P.R. China
[2]*Department of Physics and Astronomy, Drake University, Des Moines, Iowa, 50311, USA*
[3]*LPP-CNRS, Ecole Polytechnique, 91128 Palaiseau, France*
(Dated: January 17, 2013)

The *B*-spline *R*-matrix (BSR) method is employed to calculate elastic electron scattering from chlorine atoms in the $(3p^5)^2P^o_{3/2,1/2}$ states and electron-induced collisions between these two fine-structure levels. The polarizability of the target states is accounted for by including polarized pseudostates in the close-coupling expansion, while relativistic effects are treated at the level of the semirelativistic Breit-Pauli approximation. We find the Ramsauer minimum in the elastic channels at a significantly lower projectile energy ($\approx 0.2\,\mathrm{eV}$) than previous calculations, due to an apparent strong sensitivity of the theoretical predictions on the details of the model, especially the target structure. The present results are relevant to the determination of chlorine atomic densities in Cl_2-containing industrial plasma etch reactors.

PACS numbers: 34.80.Bm,34.80.Dp

I. INTRODUCTION

Chlorine-based inductively-coupled plasmas are widely used for etching of complementary metal-oxide-semiconductor (CMOS) gates for integrated circuit manufacture. A key parameter characterizing such a discharge is the density of chlorine atoms. Relative Cl atom densities can be determined by two-photon absorption laser-induced fluorescence (TALIF) with an excitation laser wavelength of 233.277 nm [1]. Recently a calibration technique was demonstrated for putting these densities on an absolute scale using $355\,\mathrm{nm}$ photolysis of Cl_2 [2]. However, this method only determines the density in the $(3p^5)^2P^o_{3/2}$ ground state, whereas a spin-orbit excited $(3p^5)^2P^o_{1/2}$ state exists at an energy of only $0.109\,\mathrm{eV}$ above the ground state [3]. If the spin-orbit distribution were in equilibrium with the electron temperature, the additional density of Cl atoms in this (unobserved) state could approach 50% of that in the ground state. There are several mechanisms, however, including quenching at the reactor walls or collisional quenching with Cl_2, that can lead to significant deviations from the equilibrium distribution. Consequently, it is necessary to have accurate cross sections available, especially for excitation of the $^2P^o_{3/2} \rightarrow\, ^2P^o_{1/2}$ transition (and the reverse process of deexcitation). These can then be used to include the $^2P^o_{1/2}$ state in plasma chemistry models such as the Hybrid Plasma Equipment Model (HPEM) [4]. Results of these studies will be reported in

a forthcoming publication [5].

The primary motivation for the work reported in this communication, therefore, was the need for the cross sections mentioned above. While earlier calculations for the e–Cl collision system are available [6–8], they were all performed with nonrelativistic models and hence are not suitable to provide data for the finestructure-resolved transition. Furthermore, there are significant differences between the various sets of results reported, especially regarding the position of the Ramsauer minimum in the elastic channel. Since this position is apparently very sensitive to the details of the model, it seemed desirable to perform another calculation to investigate the issue further.

This paper is organized as follows. After a brief overview of the computational method in Sect. II, the results are presented and discussed in Sect. III. We finish with a summary and conclusions in Sect. IV.

II. COMPUTATIONAL DETAILS

The target states of chlorine in the present calculations were generated by combining the multiconfiguration Hartree-Fock (MCHF) and the *B*-spline box-based close-coupling methods [9]. Since we are only interested in collisions involving the two states with the dominant valence configuration $3p^5$, these were the only physical states generated. On the other hand, it is well known that long-range polarization effects of the target due to the incident projectile are of critical importance particularly for elastic scattering. This effect can be simulated in a variety of ways, including semi-empirical (usually local) model potentials [6, 10, 11], continuum MCHF [8], the polarized-orbital approach [12], or coupling to specially constructed pseudostates in a close-coupling expansion [7]. Employ-

ing only a few such states, with their particular design, is a frequently taken short-cut for convergent close-coupling (CCC) [13] or R-matrix with pseudostates (RMPS) [14] calculations. Note that carrying out the latter is a very challenging endeavor [15, 16], especially for open-shell systems.

Since the polarized pseudostate approach is known to work well for low-energy elastic scattering, we applied it to the present case of interest as well. Specifically, we constructed one ^2S, ^2P, and ^2D state of even parity each to account for dipole coupling of the $^2P^o$ ground state to the entire Rydberg series as well as the ionization continuum in our nonrelativistic model. In the semi-relativistic calculation based on the Breit-Pauli hamiltonian, we constructed the corresponding $^2S_{1/2}$, $^2P_{3/2,1/2}$, and $^2D_{3/2,5/2}$ states, respectively. Details of our procduere can be found in [17]. In all models, the polarizability of the $^2P^o_{3/2,1/2}$ states, obtained *ab initio*, was about $14.0\,a_0^3$, where $a_0 = 0.529 \times 10^{-10}$ m is the Bohr radius. This is slightly less than the accepted value of about $14.7\,a_0^3$ [18].

We set up the close-coupling expansion including the above states, i.e., the $^2P^o$ ground state plus three pseudostates in the nonrelativistic case and the $^2P^o_{3/2,1/2}$ states plus six pseudostates for the Breit-Pauli case. The resulting equations were solved by means of the B-spline R-matrix (BSR) method with the suite of codes published by Zatsarinny [19]. The distinctive feature of the method is the use of B-splines as a universal basis to represent the scattering orbitals in the inner region of $r \leq a$. Furthermore, using individually optimized, and hence nonorthogonal sets of one-electron radial functions for the target states provides high flexibility and accuracy in the structure description. Furthermore, the excellent numerical properties of B-splines are advantageous in the description of the projectile.

The R-matrix radius was set to $30\,a_0$. We employed 71 B-splines of order 8 to span this radial range using a semi-exponential knot grid. The maximum interval in this grid is $0.65\,a_0$. This is sufficient to cover the electron scattering energies for which results are shown here. We calculated partial waves for angular momenta $L, J \leq 10$ by employing the FARM program [20] for the asymptotic region. No top-up procedure to account for contributions from higher partial waves was required.

III. RESULTS

Figure 1 shows the angle-integrated cross section for elastic electron scattering from chlorine atoms in the $(3p^5)^2P^o$ state. Note that a pure static-exchange model (only the $^2P^o$ state is accounted for) does not predict a Ramsauer minimum (curve "BSR"), but it apparently provides reasonable results for energies above ≈ 5 eV. Two other calculations, by Griffin *et al.* [7] and Saha [8] that account for the polarizability effects, as well as our own "HF-pol" model, in which polarized target states
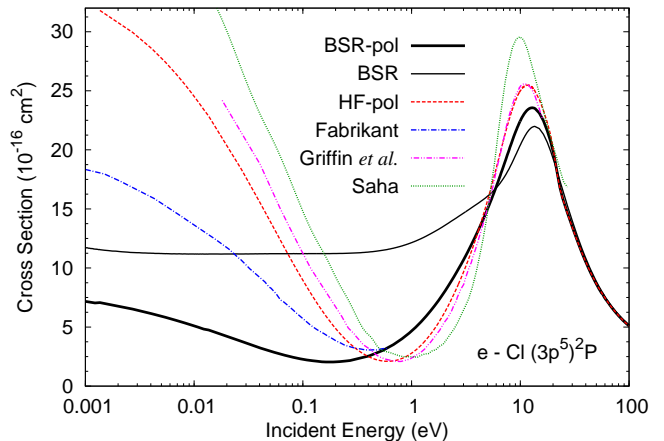

FIG. 1. (Color online) Angle-integrated cross section for elastic electron scattering from chlorine atoms in the $(3p^5)^2P^o$ state. The various models are described in the text.

were calculated at the level of the polarized Hartree-Fock approximation, yield a Ramsauer minimum around or just below an incident energy of 1 eV. These calculations also agree well with each other below and above this minimum. Fabrikant [6], on the other hand, who extrapolated parameters from a model potential approach, predicts the minimum around 0.4 eV, and our BSR-pol calculation yields an even lower energy of ≈ 0.2 eV.

Without experimental data being available for comparison, we cannot be certain regarding the actual position of the minimum, nor can we be sure regarding the value of the cross section at very low energies, where the differences between the various theoretical datasets are substantial. Increasing the correlation put into the target states (done fully *ab initio* in BSR-pol) seems to reduce the position of the minimum and also the predicted cross-section values for low incident energies.

Figure 2 exhibits the angle-integrated cross section for elastic scattering from both finestructure states, as well as for excitation and deexcitation of the $^2P^o_{3/2} \leftrightarrow^2 P^o_{1/2}$ transitions. While the results for elastic scattering depend strongly on whether or not the polarization of the target due to the incident electron is accounted for, the predictions for the inelastic/superelastic transitions are very similar for both cases. This is due to the fact that elastic scattering is often dominated by long-range interactions, while the state-changing transitions occur when the projectile is near the target. Given the stability of the latter results, we are confident that they are sufficiently accurate to be used in plasma chemistry models.

Figure 3 displays the corresponding momentum-transfer cross section, as obtained for elastic scattering in various models. Note that momentum-transfer rather than elastic cross sections are most important for plasma modeling. Not surprisingly (see also Fig. 1), Saha's continuum MCHF results are significantly different from the BSR-pol predictions at very low energies.

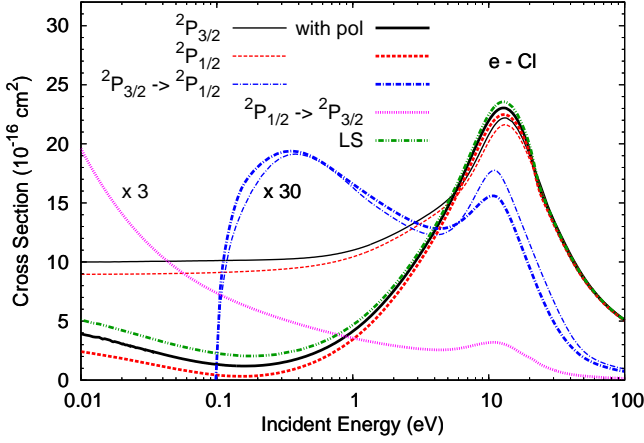Finally, a close inspection of the previous figures re-

FIG. 2. (Color online) Angle-integrated cross section for elastic electron scattering from chlorine atoms in the $(3p^5)^2P^o_{3/2}$ and $(3p^5)^2P^o_{1/2}$ states, for the inelastic $^2P^o_{3/2} \to^2 P^o_{1/2}$ transition, and the superelastic $^2P^o_{1/2} \to^2 P^o_{3/2}$ transition. The latter results have been multiplied by factors of 30 and 3, respectively, for better visibility. The thick (thin) lines correspond to results obtained with (without) the polarizability effect. The curve labeled "LS" represents the nonrelativistic results for elastic scattering.
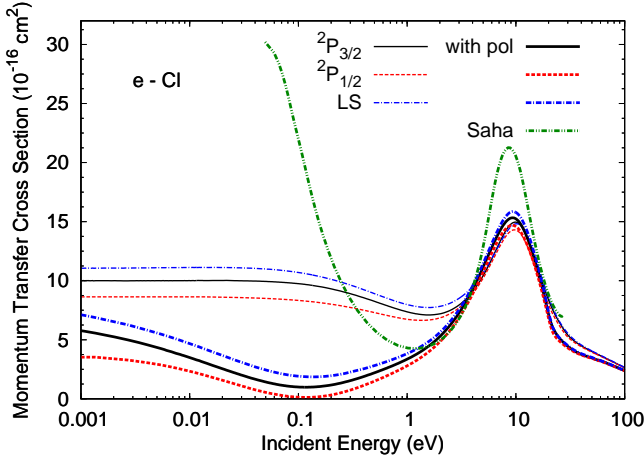

FIG. 3. (Color online) Angle-integrated elastic momentum transfer cross section for elastic electron scattering from chlorine atoms in the $(3p^5)^2P^o_{3/2}$ and $(3p^5)^2P^o_{1/2}$ states. The models are the same as those used in Fig. 2.
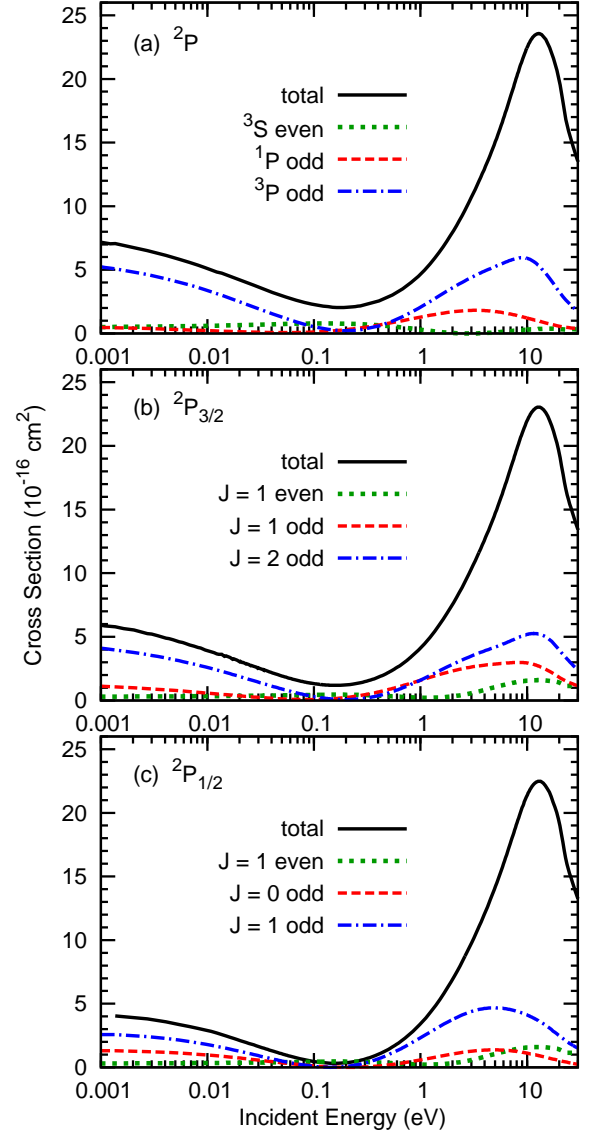

FIG. 4. (Color online) Angle-integrated cross section, and the most important partial-wave contributions, for elastic electron scattering from chlorine atoms. The top panel shows our nonrelativistic predictions, while the center and bottom panels exhibit the semirelativistic results for the $^2P^o_{3/2}$ and $^2P^o_{1/2}$ states, respectively.

veals a significant model dependence of the results in the vicinity of the Ramsauer minimum. This is analyzed in more detail for the BSR-pol predictions in Fig. 4, which shows the total cross section and its most important individual contributions. Not surprisingly, this energy range is dominated by partial waves, for which the projectile has an orbital angular momentum of $l = 0$ or $l = 1$. The former essentially determines the position of the Ramsauer minimum, while the latter mostly determines the height, although there are also significant contributions from higher partial waves, especially from $l = 2$. Note

that the nonrelativistic prediction (top panel of Fig. 4) does not lie between the results for the two individual finestructure levels. This is due to a slight change in the target description when relativistic effects are accounted for, in turn resulting in a small variation of the effective potential seen by the projectile.

In this context, a comparison of the scattering lengths is of interest as well. Table I lists the results from various models. Not surprisingly, the differences are substantial.

nonrelativistic			relativistic		
LS	BSR	Saha [8]	J^π	BSR	Fabrikant [6]
$^1P^o$	-0.857	-1.478	1°	-1.035	-1.97
$^3P^o$	-1.541	-2.707	2°	-1.495	-2.46

TABLE I. Scattering lengths from various models. The relativistic case is for the $^2P_{3/2}$ target state.

IV. SUMMARY AND CONCLUSIONS

We have presented a revised set of cross sections for elastic scattering as well as electron-induced excitation involving the ground state, $^2P^o_{3/2}$, and the first excited state, $^2P^o_{1/2}$, state of the chlorine atom. Due to the highly reactive nature of atomic chlorine, no experimental collision data are currently available to assess the validity of the various theoretical predictions. For energies above $1\,\mathrm{eV}$, our results are in good agreement with predictions from previous nonrelativistic calculations, while serious discrepancies were found in the very low-energy regime. These energies, on the other hand, are important in the modeling of low-temperature plasmas. In the particular CMOS application mentioned above, which provided the principal motivation for the present work, excitation cross sections for the inelastic $^2P^o_{3/2} \to\,^2P^o_{1/2}$ transition are required. Preliminary results suggest that the present model is, indeed, sufficient to accurately predict the relative abundance of chlorine atoms in the two fine-structure levels under various plasma conditions [5]. The semirelativistic BSR-pol data presented in this paper are available from the authors upon request.

[1] K. Ono, T. Oomori, M. Tuda, and K. Namba, Journal of Vacuum Science & Technology **10** (1992) 1071.

[2] J. P. Booth, Y. Azamoum, N. Sirse, and P. Chabert, Journal of Physics D **45** (2012) 195201.

[3] A. Kramida, Yu. Ralchenko, J. Reader, and NIST ASD team (2012), NIST Atomic Spectra Database (Version 5) http://www.nist.gov/pml/data/asd.cfm

[4] P. Subramonium and M. J. Kushner, Journal of Vacuum Science & Technology **20** (2002) 313.

[5] J. P. Booth, N. Sirse, P. Indelicato, Y. Wang, O. Zatsarinny, K. Bartschat, and M.J. Kushner, in preparation.

[6] I. I. Fabrikant, J. Phys. B **27** (1994) 4545.

[7] D. C. Griffin, M. S. Pindzola, T. W Gorczyka, and N. R. Badnell, Phys. Rev. A **51** (1995) 2265.

[8] H. P. Saha, Phys. Rev. A **53** (1996) 1553.

[9] O. Zatsarinny and C. Froese Fischer, Comp. Phys. Commun. **180**, 2041 (2009).

[10] F. Blanco and G. Garcia, Phys. Lett. **317** (2003) 458.

[11] O. Zatsarinny, K. Bartschat, G. Garcia, F. Blanco, L. R. Hargreaves, D. B. Jones, R. Murrie, J. R. Brunton, M. J. Brunger, M. Hoshino, and S. J. Buckman, Phys. Rev. A **83** (2011) 042702.

[12] R. P. McEachran and A. D. Stauffer, Austr. J. of Phys. **50** (1997) 511.

[13] I. Bray, D. V. Fursa, A. S. Kheifets, and A. T. Stelbovics, J. Phys. B **35** (2002) R117.

[14] K. Bartschat, E. T. Hudson, M. P. Scott, P. G. Burke, and V. M. Burke, J. Phys. B **29** (1996) 115.

[15] O. Zatsarinny and K. Bartschat, Phys. Rev. A **85** (2012) 062710.

[16] O. Zatsarinny and K. Bartschat, Phys. Rev. A **86** (2012) 022717.

[17] O. Zatsarinny, K. Bartschat, and M. Allan, Phys. Rev. A **83** (2011) 032713.

[18] P. Schwerdtfeger (2012), http://ctcp.massey.ac.nz/dipole-polarizabilities/

[19] O. Zatsarinny, Comp. Phys. Commun. **174** (2006) 273.

[20] V. M. Burke and C. J. Noble, Comput. Phys. Commun. **85**, 471 (1995).